



## Using of carbon nanofibers as effective scavengers for the uptake of Co(II) and Ni(II) in water by batch investigations

Qingyuan Hu<sup>a</sup>, Qingzhou Zhao<sup>b</sup>, Baowei Hu<sup>a,\*</sup>, Yuling Zhu<sup>a</sup>, Guodong Sheng<sup>a,\*</sup>, Abdullah M. Asiri<sup>c</sup>, Hadi M. Marwani<sup>c</sup>

<sup>a</sup>College of Life Science, College of Chemistry and Chemical Engineering, Shaoxing University, Zhejiang 312000, China, Fax: +86 575 8834 1521; emails: hbw@usx.edu.cn (B. Hu), gdsheng@usx.edu.cn (G. Sheng), QingyuanHu32@126.com (Q. Hu), 36030589@qq.com (Y. Zhu)

<sup>b</sup>College of Resources and Environment, University of Chinese Academy of Sciences, 19 A Yuquan Road, Beijing 100049, China, email: zqz1992@hotmail.com

<sup>c</sup>Chemistry Department, Faculty of Science, King Abdulaziz University, Jeddah 21589, Saudi Arabia, emails: aasiri2@kau.edu.sa (A.M. Asiri), hmarwani@kau.edu.sa (H.M. Marwani)

Received 5 February 2018; Accepted 3 September 2018

### ABSTRACT

Carbon nanofibers (CNFs) have been extensively investigated due to their strong uptake and complexation ability. In this work, CNFs was characterized by using SEM, TEM, FTIR, XPS and Raman spectra. The uptake of Co(II) and Ni(II) on bacterium-derived CNFs as a function of contact time, pH, ionic strength and temperature was investigated using batch techniques. The pH-dependent uptake indicated that the uptake of Co(II) and Ni(II) onto CNFs was significantly higher at high pH values than that at low pH values. The uptake of Co(II) and Ni(II) onto CNFs was hardly affected by ionic strength, suggesting the formation of inner-sphere surface complexation of Co(II) and Ni(II) onto CNFs over a wide pH range. The Langmuir model described the uptake of Co(II) and Ni(II) onto CNFs better than the other models did. According to regeneration experiments, CNFs displayed good recoverability and recyclability in the Co(II) and Ni(II) uptake process. The findings presented herein play a significant role in the scavenging of metal ions on inexpensive and available CNFs in environmental cleanup applications.

*Keywords:* Carbon nanofibers; Uptake; Scavenging; Co(II); Ni(II)

### 1. Introduction

In recent years, industrialization and urbanization has contributed to the great discharge of large amounts of heavy metals with high toxicity in the natural water and soil bodies, such as Cd(II), Hg(II), U(VI), Cu(II), Cr(VI), Zn(II), As(V)/As(III), Ni(II), Pb(II), Se(VI)/Se(IV), Co(II), and so on [1–10]. Due to the non-bioavailability, mobility and persistency in environmental systems, these metals have been considered as major pollutants which exhibited great harm to human being [1–3]. Thereby, it is critical to

develop an effective technique to remediate these metal ions from wastewater. In this respect, lots of techniques have been used for the effective scavenging of metals including adsorption, chemical reduction, membrane separation, precipitation, electrolysis, ion exchange, flocculate flotation, etc. [3–8].

Among these techniques, adsorption has been regarded as one of the main concerns due to its many advantages of low cost, easy operation and high efficiency. Therefore, in the past decades, a large number of adsorbents have been fabricated for the efficient scavenging of metal ions.

\* Corresponding authors.

These potential adsorbents included natural minerals and oxides [11–16], layered double hydroxides [17–19], titanate nanotubes [20–23], graphene oxide (GO) and its modified composites [24–33], etc. For instance, Sun et al. [27–29] have utilized raw and functionalized graphene oxides as promising adsorbents to scavenge heavy metals and radionuclides, and they reported that both GO and its functionalized composites showed amazing adsorption capacities for radionuclides such as U(VI), Eu(III) and Th(IV), due to the high specific surface area, and large amount of oxygenated functional groups. Carbon nanofibers (CNFs) with interconnected 3-D networks, an alternative to carbon-based materials, can be prepared by a facile, low cost, and environmentally friendly pyrolyzing method. Besides, CNFs presented unique properties including high porosity and specific surface area, low density as well as excellent recyclability. Recently CNFs have also been used for the cleanup of various pollutants [34–38]. Ding et al. [36] studied the competitive sorption of Pb(II), Cu(II) and Ni(II) on CNFs, and Cheng et al. [37] studied the competitive sorption of As(V) and Cr(VI) on CNFs. It was demonstrated that CNFs presented high adsorption capacity for these ions. However, few studies concerning the scavenging of heavy metals on CNFs have been reported.

Among the metal ions, cobalt element (Co(II)) is the primary constituent of vitamin B<sub>12</sub> and thus an essential nutrient for life in trace amounts. But excessive oral doses can contribute to adverse effects on human beings [39–41]. In addition, nickel element (Ni(II)) is widely used in steel factories, nickel batteries and some alloys, Ni(II) is also an important product of neutron activation of reactor materials [42–44]. So, Co(II) and Ni(II) can be easily released into the natural water and soil environment, imposing great harm to the ecosystem [39–44]. Hence, it is quite essential to remove Co(II) and Ni(II) from wastewater, which is very important to protect the environment and establish environment management systems.

Therefore, in the present paper, CNFs were used as effective scavengers for the uptake of Co(II) and Ni(II) from wastewater by batch investigations. The applicability of CNFs in the scavenging of Co(II) and Ni(II) was determined concerning the uptake kinetics and capacity, role of pH and ionic strength, as well as the regeneration and reuse. The uptake isotherm of Co(II) and Ni(II) will be fitted by different models. The uptake mechanism will be also discussed.

## 2. Materials and methods

### 2.1. Materials and chemicals

All chemicals in analytical purity were obtained from Sinopharm chemical reagent Beijing cooperation, China, and used in this experiment without further purification. All reagents were prepared with high-purity Milli-Q water obtained from a Millipore Synthesis A10 water system. The CNFs were prepared via the pyrolysis of bacterial cellulose pellicles under N<sub>2</sub> atmosphere. The morphology and nanostructure of CNFs were characterized by scanning electron microscopy (SEM) (FEI-JSM 6320F) and transmission electron microscopy (TEM) images (Hitachi H7650 transmission electron microscope). Raman spectra were recorded with a

Renishaw in Via Raman spectrometer (Renishaw plc, UK). The surface functional groups of CNFs were recorded by Fourier transformed infrared (FT-IR) (Nicolet 8700 FT-IR spectrometer) in pressed KBr pellets (Sigma-Aldrich, 99%, FT-IR grade) and X-ray photoelectron spectroscopy (XPS) (Thermo Escalab 250) [3,34].

### 2.2. Uptake procedure

The uptake procedure of Co(II) and Ni(II) on CNFs was studied using batch technique in 10-mL polyethylene centrifuge tubes. First, the stock suspension of CNFs and background electrolyte namely NaNO<sub>3</sub> solution was mixed for 1 d to get equilibrium of CNFs and background electrolyte. Then, metal ions namely Co(II) or Ni(II) stock solution were added to get the desired concentrations of different uptake systems. The uptake suspension pH was adjusted to desired values by using HNO<sub>3</sub> or NaOH with concentration of 0.01 mol/L. After the suspension was continuously rotated for 1 d to obtain uptake equilibrium, the suspension was centrifuged for 30 min, and filtered with a 0.22- $\mu$ m membrane filter, to separate the solid and liquid. The Co(II) and Ni(II) concentration were determined by atomic absorption spectrometer. The uptake of Co(II) and Ni(II) onto CNFs was calculated from the difference between initial and equilibrium concentration. The uptake percentage (uptake (%)) =  $(C_0 - C_e)/C_0 \times 100\%$  was calculated from the difference of the initial concentration ( $C_0$ ) and final concentration ( $C_e$ ) in supernatant after separation by centrifugation and filtration.

## 3. Results and discussion

### 3.1. Structural characterization

Fig. 1 displayed the morphology and nanostructure of CNFs characterized by SEM, TEM, XPS and Raman spectra. According to the SEM and TEM observations (Figs. 1(A) and (B)), the CNFs exhibited a porous interconnected 3D framework, the diameter of CNFs ranged from a few tens to hundreds of nanometers. Besides, these nanofibers were randomly oriented in 3D cross-linked graphitic layers [34]. Fig. 1(C) shows the high resolution C 1s XPS spectrum of CNFs, which can be deconvoluted into four peaks at ~284.1, 286.4, 287.3 and 289.4 eV, indicative of C–C, C–O, C=O and COO– groups, respectively. XPS analysis suggested that CNFs presented lots of oxygenated functional groups such as –OH and –COOH groups [34]. The Raman spectra of CNFs showed two clear peaks at ~1,360 and ~1,570 cm<sup>-1</sup> (Fig. 1(D)), suggesting the D band that is indicative of partially disordered structures of sp<sup>2</sup> domains, and G band that is related to the E<sub>2g</sub> vibration mode of sp<sup>2</sup> carbon domains. Compared with raw CNFs, the value of I<sub>D</sub>/I<sub>G</sub> of Co(II) and Ni(II) adsorbed CNFs decreased, demonstrating the decrease of amorphous carbon [3]. Fig. 2 shows the Fourier transform infrared (FTIR) spectrum of CNFs. The peaks at ~3,450 and ~1,760 cm<sup>-1</sup> were due to the stretching vibration of –OH and –C=O groups, respectively. Other peaks at ~2,930; 1,610; 1,400 and 1,120 cm<sup>-1</sup> were due to the stretching vibrations of C–H, C=C, C–OH and C–O–C groups, respectively [35]. This result once again proved the presence of abundant O-bearing functional groups on CNF surfaces.

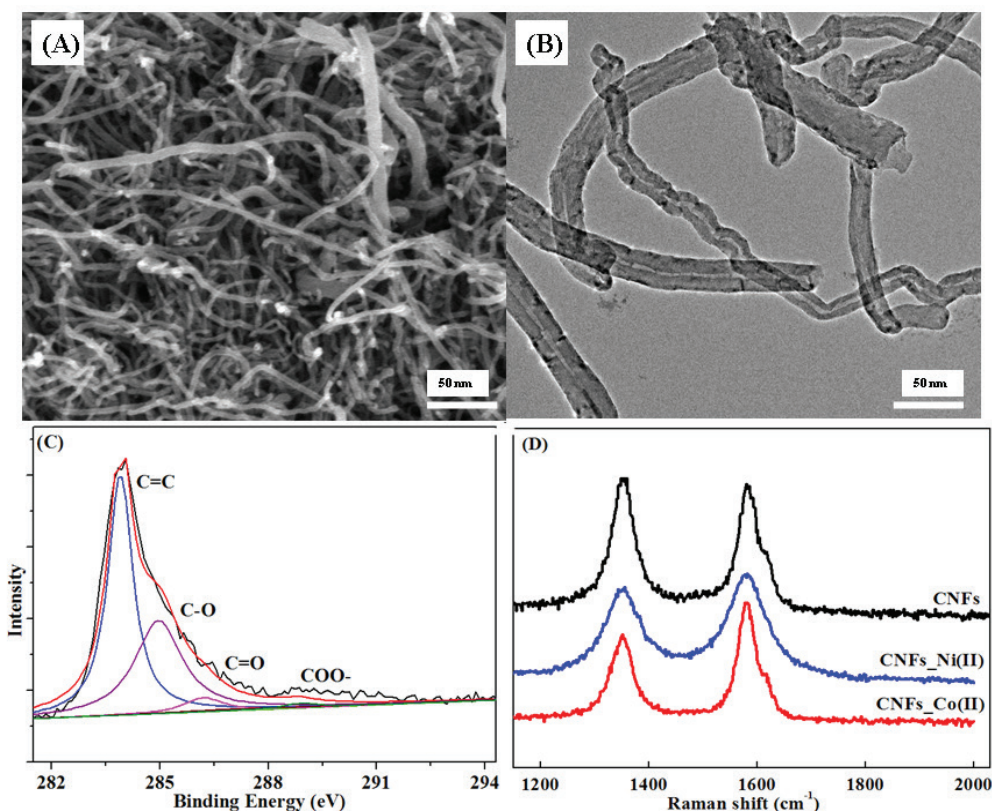


Fig. 1. Characterization results of CNFs, (A) SEM, (B) TEM, (C) C 1s of XPS spectrum, and (D) Raman spectra.

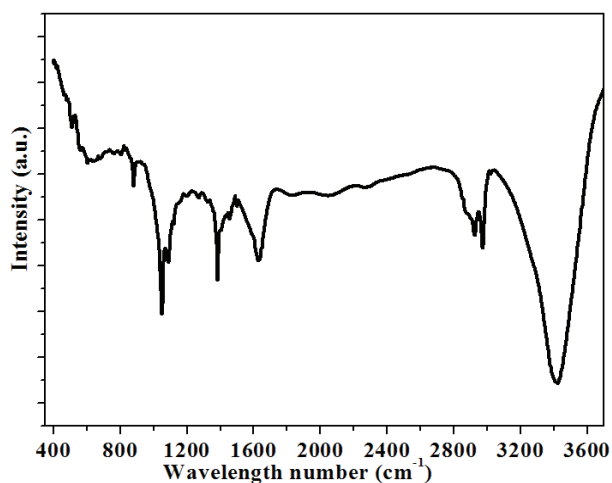


Fig. 2. Fourier transform infrared (FTIR) spectrum of CNFs.

### 3.2. Effect of equilibrium time

Fig. 3 shows the uptake of Co(II) and Ni(II) onto CNFs affected by equilibrium time. We can see that Co(II) and Ni(II) uptake onto CNFs increased rapidly at the beginning, then keeps the high level. Such a short equilibrium time suggests the presence of chemical interaction rather than physical interaction for Co(II) and Ni(II) uptake onto CNFs [39,45]. In addition, the fast uptake is attributed to the rapid migration of Co(II) and Ni(II) into the external sites of CNFs, which

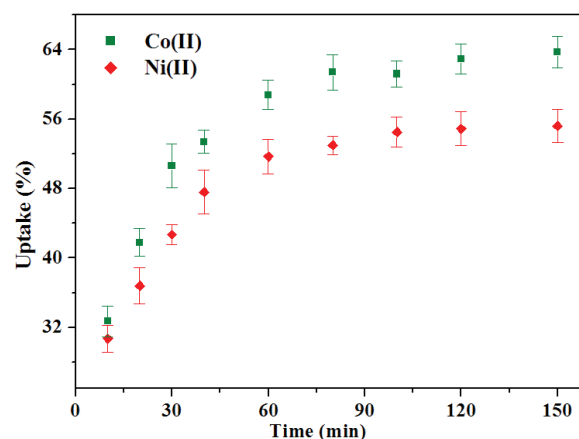


Fig. 3. Uptake kinetics of Co(II) and Ni(II) onto CNFs,  $C_0 = 10.0$  mg/L,  $I = 0.01$  mol/L NaNO<sub>3</sub>,  $T = 298$  K.

can be used for continuous effluent decontamination. Based on uptake kinetics, an equilibrium time of 1 d is selected to ensure complete uptake of Co(II) and Ni(II) onto CNFs.

### 3.3. Effect of pH

The uptake of Co(II) and Ni(II) onto CNFs affected by pH is shown in Figs. 4(A) and (B), respectively. It is clear that pH plays a central role in Co(II) and Ni(II) uptake. The uptake of Co(II) and Ni(II) onto CNFs increases from ~20%

to ~90% with pH increasing from ~2.0 to ~8.0, and finally Co(II) and Ni(II) uptake maintains high level at pH > 8.0. There are two uptake sites on CNFs, that is, protonated sites ( $\text{XOH}_2^+$ ) owing to protonation reaction ( $\text{XOH} + \text{H}^+ = \text{XOH}_2^+$ ), deprotonated sites ( $\text{XO}^-$ ) owing to deprotonation reaction ( $\text{XOH} = \text{H}^+ + \text{XO}^-$ ). The amount of protonated sites decreases but the amount of deprotonated sites increases with increase in pH [46–48]. Besides, the relative proportion of Co(II) and Ni(II) species are presented in Fig. 5. It is obvious that Co(II) and Ni(II) mainly existed as positively-charged  $\text{Co}^{2+}$  or  $\text{Ni}^{2+}$  species at low pH values [46–48]. And CNFs surfaces are positively-charged, hence, the electrostatic repulsion between  $\text{Co}^{2+}$  or  $\text{Ni}^{2+}$  and protonated sites of CNFs leads to low Co(II) and Ni(II) uptake. In contrast, CNF surfaces become negatively charged at high pH values, and electrostatic attraction between negatively charged sites and positively charged  $\text{Co}^{2+}$  or  $\text{Ni}^{2+}$  increases the uptake [46–48]. Nevertheless, at high pH values, Co(II) and Ni(II) mainly existed as  $\text{Co}(\text{OH})_2$  or  $\text{Ni}(\text{OH})_2$ , so the high uptake of Co(II) and Ni(II) onto CNFs is attributed to the formation of  $\text{Co}(\text{OH})_2$  or  $\text{Ni}(\text{OH})_2$  surface precipitates and some surface complexes.

### 3.4. Effect of ionic strength

Fig. 4 also shows the effect of ionic strength on uptake of Co(II) and Ni(II) onto CNFs using  $\text{NaNO}_3$  as background electrolytes. It is well known that  $\text{NO}_3^-$  does not form complexes with Co(II) and Ni(II) in solution or on CNFs. The effect of ionic strength on Co(II) and Ni(II) uptake onto CNFs is primarily contributed to the competition of  $\text{H}^+/\text{Na}^+$  with Co(II) or Ni(II) on CNFs. We can see that Co(II) and Ni(II) uptake is hardly influenced by ionic strength in the wide pH range. The effect of ionic strength on the adsorption of Co(II) and Ni(II) onto CNFs is consistent with the uptake of other metals onto CNFs reported in the literatures [35–37].

### 3.5. Uptake isotherms of Co(II) and Ni(II) onto CNFs

The uptake isotherms of Co(II) and Ni(II) onto CNFs at 298, 318 and 338 K are presented in Figs. 6(A) and (B), respectively. We can see from that the uptake of Co(II) and Ni(II) onto CNFs increases with increase in temperature. The uptake isotherm of Co(II) and Ni(II) onto CNFs is the

highest at  $T = 338$  K but the lowest at  $T = 298$  K, indicating that Co(II) and Ni(II) uptake onto CNFs is an endothermic process [39,45]. Herein, the Langmuir, Freundlich and Dubinin–Radushkevich (D–R) isotherm models were used to fit the uptake isotherms of Co(II) and Ni(II) onto CNFs. The Langmuir isotherm has been widely used to describe

monolayer uptake process, whose form can be represented

as,  $q = \frac{bq_{\max}C_{\text{eq}}}{1 + bC_{\text{eq}}}$ , with linear form as  $\frac{C_{\text{eq}}}{q} = \frac{1}{bq_{\max}} + \frac{C_{\text{eq}}}{q_{\max}}$ , where

$C_{\text{eq}}$  is the equilibrium concentration of metal ions (mg/L),  $q$

is the amount of metal ion adsorbed on solid (mg/g),  $q_{\max}$  is

the maximum uptake capacity (mg/g), and  $b$  (L/g) is a constant that represents the heat of uptake. The Freundlich

model is based on heterogeneity surface uptake, whose form can be represented as,  $q = k_f C_{\text{eq}}^n$ , with linear form as

$\log q = \log k_f + n \log C_{\text{eq}}$ , where  $k_f$  ( $\text{mg}^{1-n} \cdot \text{L}^n/\text{g}$ ) is the uptake capacity when metal equilibrium concentration equals to 1,

and  $n$  is the degree of dependence of uptake with metal equilibrium concentration. The D–R model is valid at low concentration and can be used to describe uptake on homogeneous

or heterogeneous surfaces. Its form is  $q = q_{\max} \exp(-\beta \varepsilon^2)$ , with linear form  $\ln q = \ln q_{\max} - \beta \varepsilon^2$ , where  $\beta$  is the activity coefficient related to mean uptake energy ( $\text{mg}^2/\text{kJ}$ ), and  $\varepsilon$  is the Polanyi

potential, which is equal to,  $\varepsilon = RT \ln \left( 1 + \frac{1}{C_{\text{eq}}} \right)$ , where  $R$  is ideal

gas constant (8.3145 J/mol·K), and  $T$  is the absolute temperature in Kelvin (K).  $E$  (kJ/mol) is defined as the free energy change, which requires transferring 1 mol of metal from

solution to solid surfaces. The relation can be described as,

$E = \frac{1}{\sqrt{2\beta}}$  [45–48].

The fitting results showed that the Langmuir isotherm model described the data better than the Freundlich and D–R models did. The value of  $k_f$  calculated from the Freundlich model is large, suggesting that CNFs has high uptake affinity toward Co(II) and Ni(II). The deviation of  $n$  from unity indicates a nonlinear uptake of Co(II) and Ni(II) onto CNFs. The magnitude of  $E$  is useful for determining the uptake mechanism. Uptake is dominated by chemical forces if  $E$  is in the range of 8–16 kJ/mol, and physical forces may affect uptake in the case of  $E < 8$  kJ/mol [48]. Herein,

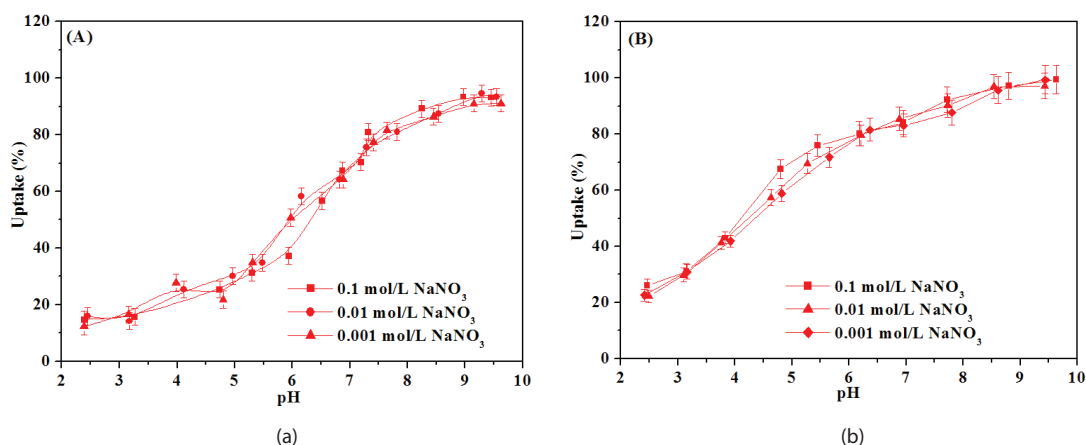


Fig. 4. Effect of pH and ionic strength on the uptake of Co(II) (A) and Ni(II) (B) onto CNFs,  $C_0 = 10.0$  mg/L,  $T = 298$  K.

the  $E$  values were determined to be higher than 8 kJ/mol, this value is in the energy range of chemical uptake process. From these analyses, we can conclude that the uptake of Co(II) and Ni(II) onto CNFs is a favorable and chemical process.

3.6. Regeneration and reuse

As more and more metal ions are released into the natural water, it is very important to treat these metal ions effectively [49–53]. For the environmental sustainability of CNFs, a high regeneration capacity would be of great value in the real wastewater treatment. In order to regenerate and reuse the CNFs after Co(II) and Ni(II) uptake. The uptake of Co(II) and Ni(II) onto CNFs decreases slightly from ~60.5% to ~58.4% after eight cycles (Fig. 7). This showed that CNFs showed a good uptake capacity and reusability. The excellent regeneration capacity indicated that CNFs can support long-term use as a cost-effective uptake material in environmental pollution control.

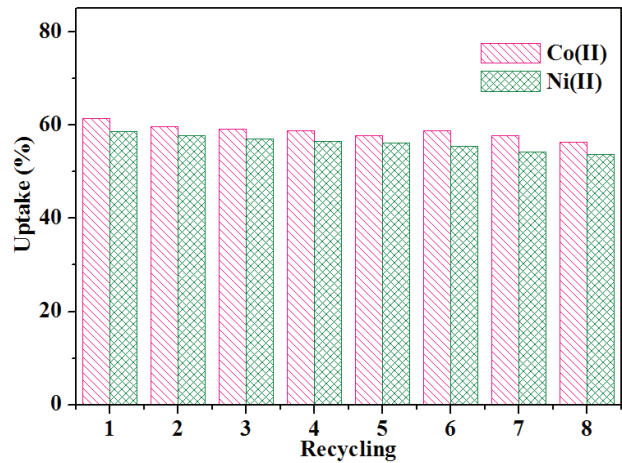


Fig. 7. Recyclability of Co(II) and Ni(II) uptake onto CNFs over eight cycles,  $C_0 = 10.0$  mg/L,  $I = 0.01$  mol/L  $\text{NaNO}_3$ ,  $T = 298$  K.

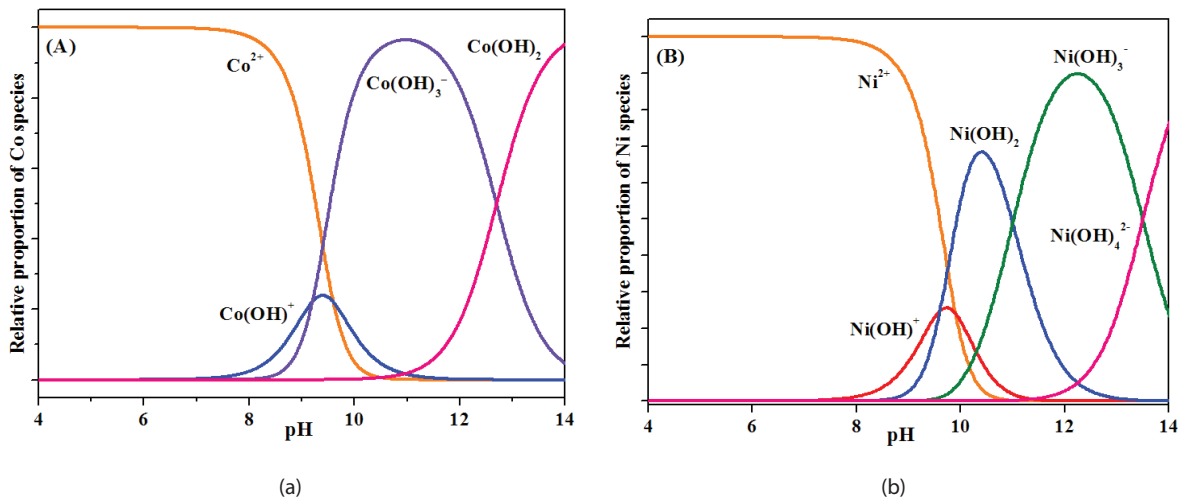


Fig. 5. Relative proportion of Co (A) and Ni (B) species in solution as a function of medium pH values.

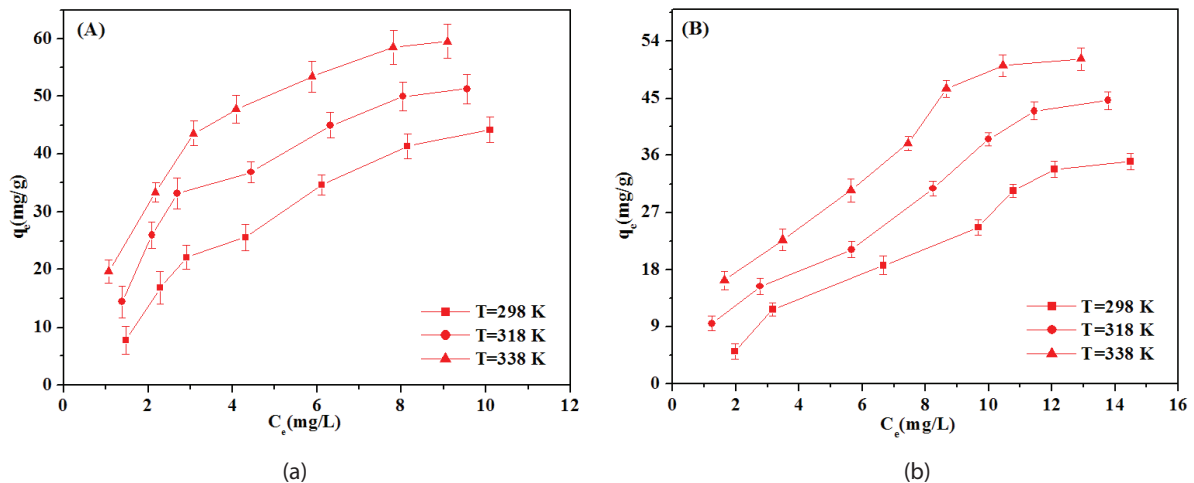


Fig. 6. Uptake isotherms of Co(II) (A) and Ni(II) (B) onto CNFs,  $I = 0.01$  mol/L  $\text{NaNO}_3$ .

#### 4. Conclusions

A batch technique was utilized to investigate the uptake of Co(II) and Ni(II) from aqueous solutions onto CNFs as a function of contact time, pH, ionic strength and temperature under ambient conditions. The results indicate that Co(II) and Ni(II) uptake onto CNFs is independent of ionic strength, indicating the formation of inner-sphere surface complexation of Co(II) and Ni(II) onto CNFs. The temperature dependent isotherm analysis suggests that the uptake process of Co(II) and Ni(II) onto CNFs is spontaneous and endothermic. Considering the low cost of CNFs, it can be regarded that CNFs showed potential application for the cost-effective remediation of Co(II)- and Ni(II)-polluted wastewaters.

#### Acknowledgments

Financial supports from China Postdoctoral Science Foundation Grant (2016M591140, 2017T100055) are acknowledged.

#### References

- [1] R. Rojas, Effect of particle size on copper removal by layered double hydroxides, *Chem. Eng. J.*, 303 (2016) 331–337.
- [2] B. Hu, F. Ye, X. Ren, D. Zhao, G. Sheng, H. Li, J. Ma, X. Wang, Y. Huang, X-ray absorption fine structure study of enhanced sequestration of U(VI) and Se(IV) by montmorillonite decorated zerovalent iron nanoparticles, *Environ. Sci. Nano*, 3 (2016) 1460–1472.
- [3] K. Chang, X. Li, B. Hu, J. Hu, G. Sheng, W. Linghu, Y. Huang, A.M. Asiri, K.A. Alamry, Molecular insights into the role of fulvic acid in cobalt sorption onto graphene oxide and reduced graphene oxide, *Chem. Eng. J.*, 327 (2017) 320–327.
- [4] G. Sheng, A. Alsaedi, W. Shammakh, S. Monaque, J. Sheng, X. Wang, H. Li, Y. Huang, Enhanced sequestration of selenite in water by nanoscale zero valent iron immobilization on carbon nanotubes by a combined batch, XPS and XAFS investigation, *Carbon*, 99 (2016) 123–130.
- [5] G. Sheng, J. Hu, H. Li, J. Li, Y. Huang, Enhanced sequestration of Cr(VI) by nanoscale zero-valent iron supported on layered double hydroxide by batch and XAFS study, *Chemosphere*, 148 (2016) 227–232.
- [6] B. Hu, C. Huang, X. Li, G. Sheng, H. Li, X. Ren, J. Ma, J. Wang, Y. Huang, Macroscopic and spectroscopic insights into the mutual interaction of graphene oxide, Cu(II), and Mg/Al layered double hydroxides, *Chem. Eng. J.*, 313 (2017) 527–534.
- [7] B. Hu, G. Chen, C. Jin, J. Hu, C. Huang, J. Sheng, G. Sheng, J. Ma, Y. Huang, Macroscopic and spectroscopic studies of the enhanced scavenging of Cr(VI) and Se(VI) from water by titanate nanotube anchored nanoscale zero-valent iron, *J. Hazard. Mater.*, 336 (2017) 214–221.
- [8] T.A. Duster, J.E.S. Szymanowski, C. Na, A.R. Showalter, B.A. Bunker, J.B. Fein, Surface complexation modeling of proton and metal sorption onto graphene oxide, *Colloids Surf., A*, 466 (2015) 28–39.
- [9] G. Sheng, P. Yang, Y. Tang, Q. Hu, H. Li, X. Ren, B. Hu, X. Wang, Y. Huang, New insights into the primary roles of diatomite in the enhanced sequestration of  $\text{UO}_2^{2+}$  by zerovalent iron nanoparticles: an advanced approach utilizing XPS and EXAFS, *Appl. Catal., B*, 193 (2016) 189–197.
- [10] K. Chang, Y. Sun, F. Ye, X. Li, G. Sheng, D. Zhao, W. Linghu, H. Li, J. Liu, Macroscopic and molecular study of the sorption and co-sorption of graphene oxide and Eu(III) onto layered double hydroxides, *Chem. Eng. J.*, 325 (2017) 665–671.
- [11] B. Hu, Q. Hu, D. Xu, C. Chen, Macroscopic and microscopic investigation on adsorption of Sr(II) on sericite, *J. Mol. Liq.*, 225 (2017) 563–568.
- [12] P. Mandaliev, T. Stumpf, J. Tits, R. Dähn, C. Walther, E. Wieland, Uptake of Eu(III) by 11 Å tobermorite and xonotlite: a TRLS and EXAFS study, *Geochim. Cosmochim. Acta*, 75 (2011) 2017–2029.
- [13] B. Hu, Q. Hu, C. Chen, Y. Sun, D. Xu, G. Sheng, New insights into Th(IV) speciation on sepiolite: evidence for EXAFS and modeling investigation, *Chem. Eng. J.*, 322 (2017) 66–72.
- [14] L. Xu, T. Zheng, S. Yang, L. Zhang, J. Wang, W. Liu, L. Chen, J. Diwu, Z. Chai, S. Wang, Uptake mechanisms of Eu(III) on hydroxyapatite: a potential permeable reactive barrier backfill material for trapping trivalent minor actinides, *Environ. Sci. Technol.*, 50 (2016) 3852–3859.
- [15] G. Sheng, S. Yang, Y. Li, X. Gao, Y. Huang, X. Wang, Retention mechanisms and microstructure of Eu(III) on manganese dioxide studied by batch and high resolution EXAFS technique, *Radiochim. Acta*, 102 (2014) 155–167.
- [16] B. Hu, W. Cheng, H. Zhang, G. Sheng, Sorption of radionickel to goethite: effect of water quality parameters and temperature, *J. Radioanal. Nucl. Chem.*, 285 (2010) 389–398.
- [17] F.R. Peligro, I. Pavlovic, R. Rojas, C. Barriga, Removal of heavy metals from simulated wastewater by in situ formation of layered double hydroxides, *Chem. Eng. J.*, 306 (2016) 1035–1040.
- [18] D. Zhao, G. Sheng, J. Hu, C. Chen, X. Wang, The adsorption of Pb(II) on Mg<sub>2</sub>Al layered double hydroxide, *Chem. Eng. J.*, 171 (2011) 167–174.
- [19] K.H. Goh, T.T. Lim, Z. Dong, Application of layered double hydroxides for removal of oxyanions: a review, *Water Res.*, 42 (2008) 1343–1368.
- [20] G. Sheng, H. Dong, R. Shen, Y. Li, Microscopic insights into the temperature-dependent adsorption of Eu(III) onto titanate nanotubes studied by FTIR, XPS, XAFS and batch technique, *Chem. Eng. J.*, 217 (2013) 486–494.
- [21] G. Sheng, L. Ye, Y. Li, H. Dong, H. Li, X. Gao, Y. Huang, EXAFS study of the interfacial interaction of nickel(II) on titanate nanotubes: role of contact time, pH and humic substances, *Chem. Eng. J.*, 248 (2014) 71–78.
- [22] G. Sheng, B. Hu, Role of solution chemistry on the trapping of radionuclide Th(IV) using titanate nanotubes as an efficient adsorbent, *J. Radioanal. Nucl. Chem.*, 298 (2013) 455–464.
- [23] G. Sheng, J. Hu, A. Alsaedi, W. Shammakh, S. Monaque, F. Ye, H. Li, Y. Huang, A.S. Alshomrani, T. Hayat, B. Ahmad, Interaction of uranium(VI) with titanate nanotubes by macroscopic and spectroscopic investigation, *J. Mol. Liq.*, 212 (2015) 563–568.
- [24] A.Y. Romanchuk, A.S. Slesarev, S.N. Kalmykov, D.V. Kosynkin, J.M. Tour, Graphene oxide for effective radionuclide removal, *Phys. Chem. Chem. Phys.*, 15 (2013) 2321–2327.
- [25] B. Hu, Q. Hu, X. Li, H. Pan, X. Tang, C. Chen, C. Huang, Rapid and highly efficient removal of Eu(III) from aqueous solutions using graphene oxide, *J. Mol. Liq.*, 229 (2017) 6–14.
- [26] Y. Xie, E.M. Helvenston, L.C. Shuller-Nickles, B.A. Powell, Surface complexation modeling of Eu(III) and U(VI) interactions with graphene oxide, *Environ. Sci. Technol.*, 50 (2016) 1821–1827.
- [27] Y. Sun, X. Wang, W. Song, S. Lu, C. Chen, X. Wang, Mechanistic insights into the decontamination of Th(IV) on graphene oxide-based composites by EXAFS and modeling techniques, *Environ. Sci. Nano*, 4 (2017) 222–232.
- [28] Y. Sun, D. Shao, C. Chen, S. Yang, X. Wang, Highly efficient enrichment of radionuclides on graphene oxide-supported polyaniline, *Environ. Sci. Technol.*, 47 (2013) 9904–9910.
- [29] Y. Sun, S. Yang, Y. Chen, C. Ding, W. Cheng, X. Wang, Adsorption and desorption of U(VI) on functionalized graphene oxides: a combined experimental and theoretical study, *Environ. Sci. Technol.*, 49 (2015) 4255–4262.
- [30] S. Chappa, A.K. Singha Deb, Sk. Musharaf Ali, A.K. Debnath, D.K. Aswal, A.K. Pandey, Change in the affinity of ethylene glycol methacrylate phosphate monomer and its polymer anchored on a graphene oxide platform toward uranium(VI) and plutonium(IV) ions, *J. Phys. Chem. B*, 120 (2016) 2942–2950.
- [31] W. Linghu, H. Yang, Y. Sun, G. Sheng, Y. Huang, One-pot synthesis of LDH/GO composites as highly effective adsorbents for decontamination of U(VI), *ACS Sustain. Chem. Eng.*, 5 (2017) 5608–5616.

- [32] B. Hu, M. Qiu, Q. Hu, Y. Sun, G. Sheng, J. Hu, J. Ma, Decontamination of Sr(II) on magnetic polyaniline/graphene oxide composites: Evidence from experimental, spectroscopic and modeling investigation, *ACS Sustain. Chem. Eng.*, 5 (2017) 6924–6931.
- [33] A.A. Kadam, J. Jang, D.S. Lee, Facile synthesis of pectin-stabilized magnetic graphene Prussian blue nanocomposites for selective cesium removal from aqueous solution, *Bioresour. Technol.*, 216 (2016) 391–398.
- [34] Y. Sun, Z. Wu, X. Wang, C. Ding, W. Cheng, S. Yu, X. Wang, Macroscopic and microscopic investigation of U(VI) and Eu(III) adsorption on carbonaceous nanofibers, *Environ. Sci. Technol.*, 50 (2016) 4459–4467.
- [35] B. Hu, Q. Hu, D. Xu, C. Chen, The adsorption of U(VI) on carbonaceous nanofibers: a combined batch, EXAFS and modeling techniques, *Sep. Purif. Technol.*, 175 (2017) 140–146.
- [36] C. Ding, W. Cheng, X. Wang, Z. Wu, Y. Sun, C. Chen, X. Wang, S. Yu, Competitive sorption of Pb(II), Cu(II) and Ni(II) on carbonaceous nanofibers: a spectroscopic and modeling approach, *J. Hazard. Mater.*, 313 (2016) 253–261.
- [37] W. Cheng, C. Ding, X. Wang, Z. Wu, Y. Sun, S. Yu, T. Hayat, X. Wang, Competitive sorption of As(V) and Cr(VI) on carbonaceous nanofibers, *Chem. Eng. J.*, 293 (2016) 311–318.
- [38] H.W. Liang, X. Cao, W.J. Zhang, H.T. Lin, F. Zhou, L.F. Chen, S.H. Yu, Robust and highly efficient free-standing carbonaceous nanofiber membranes for water purification, *Adv. Funct. Mater.*, 21 (2011) 3851–3858.
- [39] G. Sheng, H. Dong, Y. Li, Characterization of diatomite and its application for the retention of radiocobalt: role of environmental parameters, *J. Environ. Radioact.*, 113 (2012) 108–115.
- [40] M.C. Liu, C.L. Chen, J. Hu, X.L. Wu, X.K. Wang, Synthesis of magnetite/graphene oxide composite and application for cobalt(II) removal, *J. Phys. Chem. C*, 115 (2011) 25234–25240.
- [41] X. Liu, Y. Huang, S. Duan, Y. Wang, J. Li, Y. Chen, T. Hayat, X. Wang, Graphene oxides with different oxidation degrees for Co(II) ion pollution management, *Chem. Eng. J.*, 302 (2016) 763–772.
- [42] S. Yang, X. Ren, G. Zhao, W. Shi, G. Montavon, B. Grambow, X. Wang, Competitive sorption and selective sequence of Cu(II) and Ni(II) on montmorillonite: batch, modeling, EPR and XAFS studies, *Geochim. Cosmochim. Acta*, 166 (2015) 129–145.
- [43] Y. Chen, W. Zhang, S. Yang, A. Hobiny, A. Alsaedi, X. Wang, Understanding the adsorption mechanism of Ni(II) on graphene oxides by batch experiments and density functional theory studies, *Sci. China Chem.*, 59 (2016) 412–419.
- [44] G. Sheng, R. Shen, H. Dong, Y. Li, Colloidal diatomite, radionickel and humic substance interaction: a combined batch, XPS and EXAFS investigation, *Environ. Sci. Pollut. Res.*, 20 (2013) 3708–3717.
- [45] B. Hu, W. Cheng, H. Zhang, S. Yang, Solution chemistry effects on sorption behavior of radionuclide  $^{63}\text{Ni(II)}$  in illite–water suspensions, *J. Nucl. Mater.*, 406 (2010) 263–270.
- [46] X. Zhang, Y. Wang, S. Yang, Simultaneous removal of Co(II) and 1-naphthol by core-shell structured  $\text{Fe}_3\text{O}_4$ @cyclodextrin magnetic nanoparticles, *Carbohydr. Polym.*, 114 (2014) 521–529.
- [47] Z.Q. Guo, Y. Li, S.W. Zhang, H.H. Niu, Z.S. Chen, J.Z. Xu, Enhanced sorption of radiocobalt from water by Bi(III) modified montmorillonite: a novel adsorbent, *J. Hazard. Mater.*, 192 (2011) 168–175.
- [48] Q. Fu, X. Zhou, L. Xu, B. Hu, Fulvic acid decorated  $\text{Fe}_3\text{O}_4$  magnetic nanocomposites for the highly efficient sequestration of Ni(II) from an aqueous solution, *J. Mol. Liq.*, 208 (2015) 92–98.
- [49] S. Yu, X. Wang, H. Pang, R. Zhang, W. Song, D. Fu, T. Hayat, X. Wang, Boron nitride-based materials for the removal of pollutants from aqueous solutions: a review, *Chem. Eng. J.*, 333 (2018) 343–360.
- [50] J. Li, X. Wang, G. Zhao, C. Chen, Z. Chai, A. Alsaedi, T. Hayat, X. Wang, Metal-organic framework-based materials: superior adsorbents for the capture of toxic and radioactive metal ions, *Chem. Soc. Rev.*, 47 (2018) 2322–2356.
- [51] Y. Sun, S. Lu, X. Wang, C. Xu, J. Li, C. Chen, J. Chen, T. Hayat, A. Alsaedi, N.S. Alharbi, X. Wang, Plasma-facilitated synthesis of amidoxime/carbon nanofiber hybrids for effective enrichment of  $^{238}\text{U(VI)}$  and  $^{241}\text{Am(III)}$ , *Environ. Sci. Technol.*, 51 (2017) 12274–12282.
- [52] L. Yin, P. Wang, T. Wen, S. Yu, X. Wang, T. Hayat, A. Alsaedi, X. Wang, Synthesis of layered titanate nanowires at low temperature and their application in efficient removal of U(VI), *Environ. Pollut.*, 226 (2017) 125–134.
- [53] W. Yao, J. Wang, P. Wang, X. Wang, S. Yu, Y. Zou, J. Hou, T. Hayat, A. Alsaedi, X. Wang, Synergistic coagulation of GO and secondary adsorption of heavy metal ions on Ca/Al layered double hydroxides, *Environ. Pollut.*, 229 (2017) 827–836.